bourhood. And, of course, the use of high-precision astrometric measurements with instruments like the VLTI or the Keck interferometer will survey "nearby" stars for long-period systems. Altogether, these coming observational facilities will definitely help us to construct a new and more complete view of how planetary systems are born and how they evolve.

References

Boss A.P., 1997, *Science* **276**, 1836.
Charbonneau D., Brown T.M., Latham D.W., Mayor M., 2000, *ApJ* **529**, L45.
Goldreich P., Tremaine S., 1980, *ApJ* **241**, 425.
Israelian G., Santos N.C., Mayor M., Rebolo R., 2001, *Nature* **411**, 163.
Jorissen A., Mayor M., Udry S., 2001, *A&A* **379**, 992.
Mayor M., Queloz D., 1995, *Nature* **378**, 355.
Pollack J.B., Hubickyj O., Bodenheimer P., Lissauer J.J., Podolak M., Greenzweig Y., 1996, *Icarus* **124**, 62.
Saar S.H., Donahue R.A., 1997, *ApJ* **485**, 319.
Santos N.C., Israelian G., Mayor M., 2001, *A&A* **373**, 1019.
Wolszczan A., Frail D. A., 1992, *Nature* **355**, 145.

FIRES: Ultradeep Near-Infrared Imaging with ISAAC of the Hubble Deep Field South

I. LABBÉ[1], M. FRANX[1], E. DADDI[3], G. RUDNICK[2], P.G. VAN DOKKUM[4], A. MOORWOOD[3], N.M. FÖRSTER SCHREIBER[1], H.-W. RIX[5], P. VAN DER WERF[1], H. RÖTTGERING[1], L. VAN STARKENBURG[1], A. VAN DE WEL[1], I. TRUJILLO[5], and K. KUIJKEN[1]

[1]Leiden Observatory, Leiden, The Netherlands; [2]MPA, Garching, Germany; [3]ESO, Garching, Germany; [4]Caltech, Pasadena (CA), USA; [5]MPIA, Heidelberg, Germany

1. Introduction

Between October 1999 and October 2000 an undistinguished high-galactic latitude patch of sky, the Hubble Deep Field South (HDF-S), was observed with the VLT for more than 100 hours under the best seeing conditions. Using the near-infrared (NIR) imaging mode of the Infrared Spectrometer and Array Camera (ISAAC, Moorwood 1997), we obtained ultradeep images in the J_s (1.24 μm), H (1.65 μm) and K_s (2.16 μm) bands. The combined power of an 8-metre-class telescope and the high-quality wide-field imaging capabilities of ISAAC resulted in the deepest ground-based NIR observations to date, and the deepest K_s-band in any field. The first results are spectacular, demonstrating the necessity of this deep NIR imaging, and having direct consequences for our understanding of galaxy formation.

The rest-frame optical light emitted by galaxies beyond $z \sim 1$ shifts into the near-infrared. Thus, if we want to compare $1 < z < 4$ galaxies to their present-day counterparts at similar intrinsic wavelengths – in order to understand their ancestral relation – it is essential to use NIR data to access the rest-frame optical. Here, long-lived stars may dominate the total light of the galaxy and the complicating effects of active star formation and dust obscuration are less important than in the rest-frame ultraviolet. This therefore provides a better indicator of the amount of stellar mass that has formed. Compared to the selection of high-redshift galaxies by their rest-frame UV light, such as in surveys of Lyman Break Galaxies (LBGs, Steidel et al. 1996a,b),

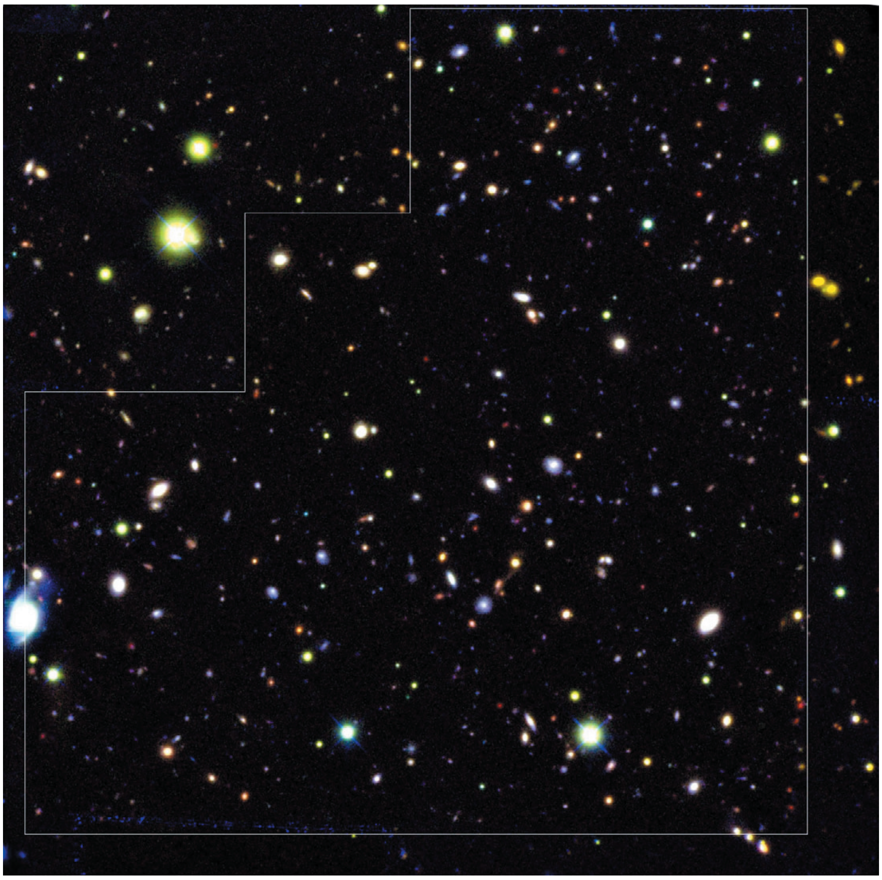

Figure 1: Three-colour composite image of the ISAAC field on top of the WFPC2 main-field, outlined in white, and parts of three WFPC2 flanking fields. The field of view is approximately 2.5 × 2.5 arcminutes and North is up. The images are registered and smoothed to a common seeing of FWHM ≈ 0.46″, coding WFPC2 I_{814} in blue, ISAAC J_s in green and ISAAC K_s in red. There is a striking variety in optical-to-infrared colours, especially for fainter objects. A number of red sources have photometric redshifts $z > 2$ and are candidates for relatively massive, evolved galaxies. These galaxies would not be selected by the U-dropout technique because they are too faint in the observer's optical.

selection in the NIR K_s-band gives a more complete census of the galaxies that contribute to the stellar mass content of the early universe. And, by studying these systems over a substantial redshift range, we can directly see how they were assembled as we look further back in time. Very deep optical-to-infrared data in many filters are required not only to access the rest-frame optical light of galaxies and constrain their stellar composition, but also to determine the redshifts of faint distant galaxies from their broad-band photometry alone. The majority of the galaxies detected are too faint to be observed spectroscopically, even with powerful telescopes like the VLT.

Here, we discuss the full NIR data set of the HDF-S. The observations, reduction techniques, the catalogue of sources, and the photometric redshifts are described in detail in Labbé et al. (2002). Throughout, we will assume a flat Λ-dominated cosmology ($\Omega_M = 0.3$, $\Lambda = 0.7$, $H_0 = 100h$ km s^{-1} Mpc^{-1}) and all magnitudes are expressed in the Johnson photometric system unless explicitly indicated by the subscript *AB* for the AB magnitude system.

2. Observations

The observations of the HDF-S are part of the Faint InfraRed Extragalactic Survey (FIRES, Franx et al. 2000), a large public programme carried out at the VLT consisting of very deep NIR ISAAC observations of two selected fields with existing deep optical WFPC2 imaging. The second and somewhat shallower field around the $z \approx 0.83$ cluster MS1054-03 (Förster Schreiber et al. in preparation) was observed for 80 hours over an area four times larger than the HDF-S. The full NIR data set of the HDF-S consists of 33.6 hours of imaging in J_s, 32.3 hours in H, and 35.6 hours in K_s with ISAAC, which has a $2.5' \times 2.5'$ field of view. The effective seeing in the reduced images is approximately 0.46″ in all bands, close to the best seeing that can be reasonably obtained from Paranal. We reach a depth of 25.9 in J_s, 24.8 in H, and 24.4 in K_s (total magnitude for point sources, 3σ). Complemented by ultradeep HST/WFPC2 imaging (version 2, Casertano et al. 2000) in the optical filters U_{300}, B_{450}, V_{606}, and I_{814} bands (the subscript indicating the effective wavelength), we assembled a K_s-selected catalogue containing 833 sources, of which 624 have seven-band photometry, covering 0.3–2.2 µm. We determined the photometric redshifts of all extragalactic sources using a method detailed in Rudnick et al. (2001, 2002a in preparation). Comparison with spectroscopic redshifts available for 49 sources in the field shows excellent agreement: $|z_{spec} - z_{phot}| / (1+z_{spec}) \approx 0.08$.

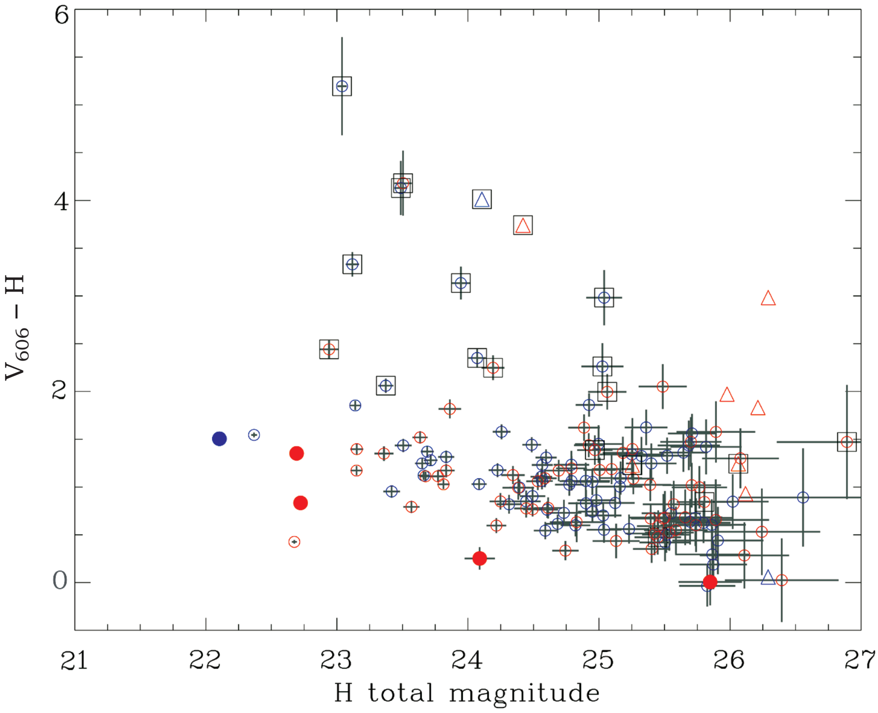

Figure 2: $V_{606} - H$ versus H colour-magnitude diagram (on the AB system) for galaxies in the HDFS K_s-selected catalogue with $1.95 < z_{phot} < 3.5$. Filled symbols indicate galaxies with spectroscopy and the data points are grouped into two redshift ranges: $1.95 \le z < 2.7$ (red) and $2.7 \le z \le 3.5$ (blue). We find 7 galaxies redder than $V_{606,AB} - H_{AB} > 3$ and brighter than $H_{AB} < 25$, compared to only one in the HDF-N. Galaxies with S/N < 2 for the V_{606} measurement (triangles) are plotted at the 2σ confidence limit in V_{606}, indicating a lower limit on the $V_{606} - H$ colour. Galaxies having red $(J_s - K_s)_J > 2.3$ colours (open squares) are also shown. The number of candidates for red, evolved galaxies is much higher than in the HDF-N for a similar survey area, as shown in an identical plot in Figure 1 of Papovich, Dickinson & Ferguson (2001). The transformation of the $V_{606} - H_s$ colour from the AB system to the Johnson magnitude system is $(V_{606} - H)_J = (V_{606} - H)_{AB} + 1.26$.

The colour image shown in Figure 1 combines HST I-band data with ISAAC data in the J_s and K_s bands. Most sources visible are very faint distant galaxies and a rich variety in their optical-to-infrared colours is readily apparent. Some high-redshift galaxies, visible as red sources, are hardly detected or even absent in the optical I-band but are quite bright in the NIR K_s.

3. Evolved Galaxies at High Redshift

Remarkably, the HDF-S contains many high-redshift sources that are relatively bright in the infrared and extremely faint in the optical, whereas the HDF-N contains far fewer such galaxies. This is clearly visible in Figure 2, which shows $V_{606} - H$ colours versus the infrared H band magnitudes of NIR selected galaxies between redshifts $2 < z < 3.5$. The filters are chosen to match those used in Figure 1 in Papovich, Dickinson & Ferguson (2001), allowing a direct comparison with the HDF-N. For a similar survey area and similar limiting depth, we find 7 galaxies redder than $V_{606,AB} - H_{AB} > 3$ and brighter than $H_{AB} < 25$ (on the AB magnitude system), compared to one in the NIR sample of HDF-N. These systems are probable candidates for relatively massive and evolved galaxies with comparatively low star-formation rates, and models of galaxy formation must allow for their formation in sufficient numbers at $z \sim 3$. It appears that in recent hydrodynamical simulations (Weinberg, Hernquist & Katz 2002) high-redshift galaxies are converting gas into stars continuously and at a fairly high rate, keeping them blue or “unevolved”. While this is qualitatively consistent with the lack of red galaxies in the HDF-N, the situation in the HDF-S is significantly different.

All high-redshift galaxies with very red $V_{606} - H$ colours also have very red infrared $J_s - K_s$ colours. Redshifting model spectra of galaxies shows that such red colours are produced by evolved systems at redshifts $z > 2$. In our K_s-band selected catalogue we find 13 relatively bright galaxies ($K_{tot} < 22$) that have red $J_s - K_s > 2.3$ colours (Franx et al. in preparation), compared to 37 U-dropouts to the same flux limit. The photometric redshifts of these galaxies, determined from the optical-to-infrared spectral energy distributions (SEDs), are between $2 < z_{phot} < 4$. Yet, most of the red galaxies are so faint in the observers optical that they would be missed by standard optical selection criteria, such as the U-dropout method. In principle, the red colours can be

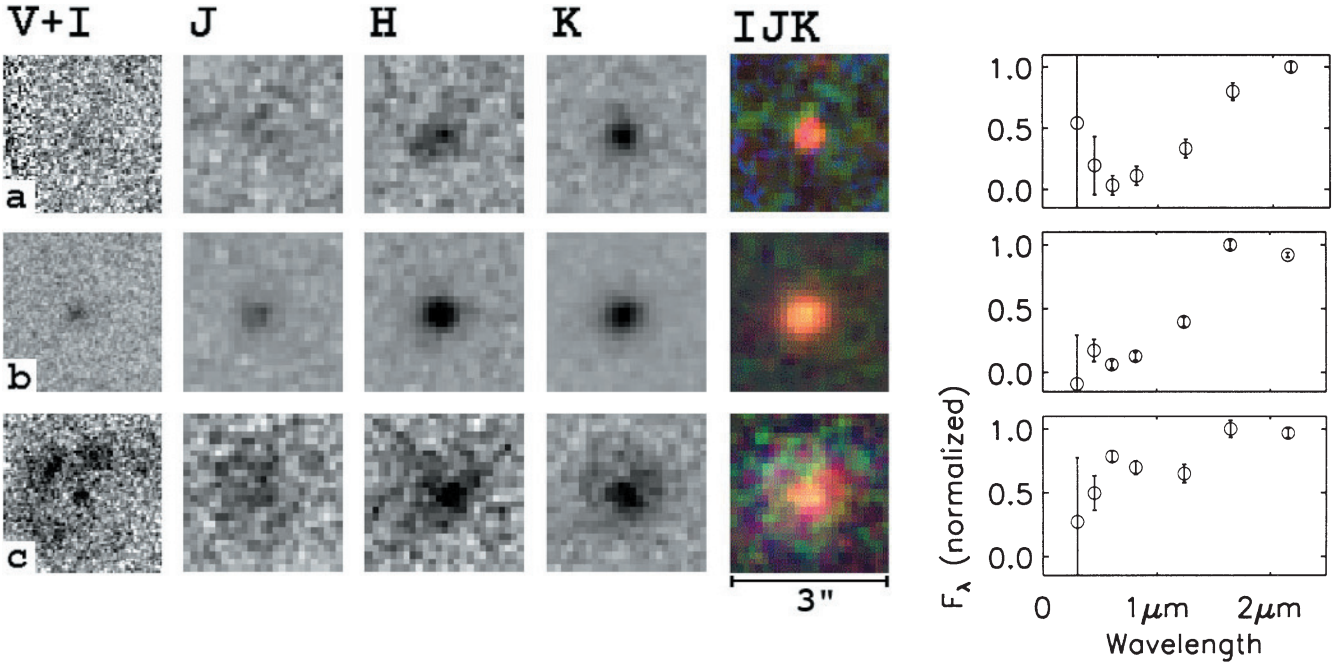

Figure 3: Morphology of bright red $J_s - K_s > 2.3$ galaxies in the HDF-S. The left grayscale panels show the averaged WFPC2 V+ I data, and right-hand panels show our VLT/ISAAC J_s, H, K_s data. The intensity is proportional to F_λ, with arbitrary normalization for each galaxy. The colour images show a combination of I, J_s, K_s data, after matching the image quality to that of the K_s-band. The right-hand column shows the spectral energy distributions. Many of these galaxies are small and show prominent breaks in the infrared (rest-frame optical). Note that the galaxy in the top row is barely visible even in J_s. The SED of the object in the middle is consistent with a strong Balmer/4000Å break at z ~ 2.5. The galaxy in the bottom row is very extended in the rest-frame optical. It shows faint emission in the H-band out to 1″, consistent with an exponential profile.

caused by dust, by contribution of prominent emission lines falling in the K_s-band, or by the redshifted Balmer or 4000 Å break, which indicates the presence of evolved stars. Although emission lines have been detected in spectroscopically confirmed $J_s - K_s > 2.3$ galaxies in the FIRES MS1054-03 field by van Dokkum et al. (in preparation), their contribution to the broadband NIR photometry is estimated to be small. In many cases the spectral energy distributions show a clear break between J_s and K_s, which is more easily explained as an aging effect than as a result of dust reddening. These galaxies contribute significantly to the rest-frame optical luminosity density (Rudnick et al. 2002a in preparation) and from their red rest-frame optical colours – implying high mass-to-light ratios – we estimate that they contain a substantial fraction of the total stellar mass present in all galaxies at $z \sim 3$.

The morphologies of the red galaxies are generally very compact at all wavelengths, as can be seen in Figure 3. A notable exception is the galaxy in Figure 3c which is clearly extended and has an exponentially decreasing surface brightness profile out to 1″ radius in the *H*-band. This galaxy seems to host blue knots which could form a spiral arm in the optical WFPC2 images, while it has an extended disk-like appearance with a prominent bulge in the centre in the ISAAC *H* and K_s images; possibly these are actively star-forming sites embedded in a larger mature host galaxy.

4. Strong Clustering of Faint Red Galaxies at $2 < z_{phot} < 4$

Presumably, high-redshift galaxies with red $J_s - K_s$ colours are among the oldest and most massive galaxies at their cosmic epoch and they have formed at the highest density peaks in the matter distribution at significantly earlier times. If so, this population should be more clustered than less massive and less evolved (bluer) objects at similar redshifts. Using the FIRES data of the HDF-S, Daddi et al. (2002) have studied the clustering behaviour of K_s-selected galaxies at $2 < z_{phot} < 4$, finding that the amount of clustering depends strongly on the $J_s - K_s$ colour of galaxies , with red galaxies more clustered than blue galaxies, very similar to what is observed in the optical in the local universe. Dividing the sample at $J_s - K_s = 1.7$ in two subsamples reveals that the galaxies with $J_s - K_s > 1.7$ colours have the largest-ever level of clustering measured for $z > 2$ galaxies (see Fig. 4). The derived correlation length for the faint red galaxies is $r_0 = 8.3 \pm 1.2$ Mpc (comoving): a factor of 3–4 higher than that of Lyman

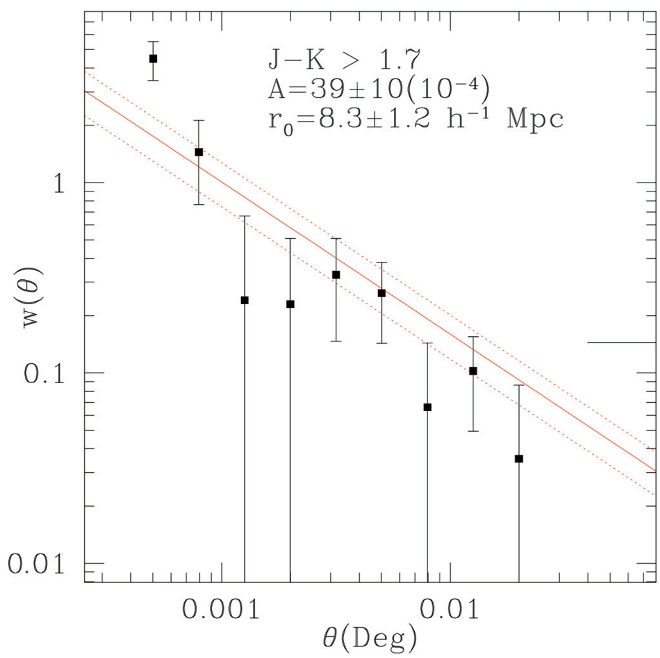

Figure 4: The angular two-point correlation function for galaxies with red $J_s - K_s > 1.7$ colours between redshifts of 2 and 4, with the best fitting power-law (solid line) and 1-sigma errors (dotted lines). A positive and large clustering signal is detected, suggesting that these red FIRES galaxies are strongly clustered in real space, with a correlation length $r_0 = 8.3 \pm 1.2\ h^{-1}$ Mpc comoving. This is the largest level of clustering ever found for distant, z > 2 galaxy populations.

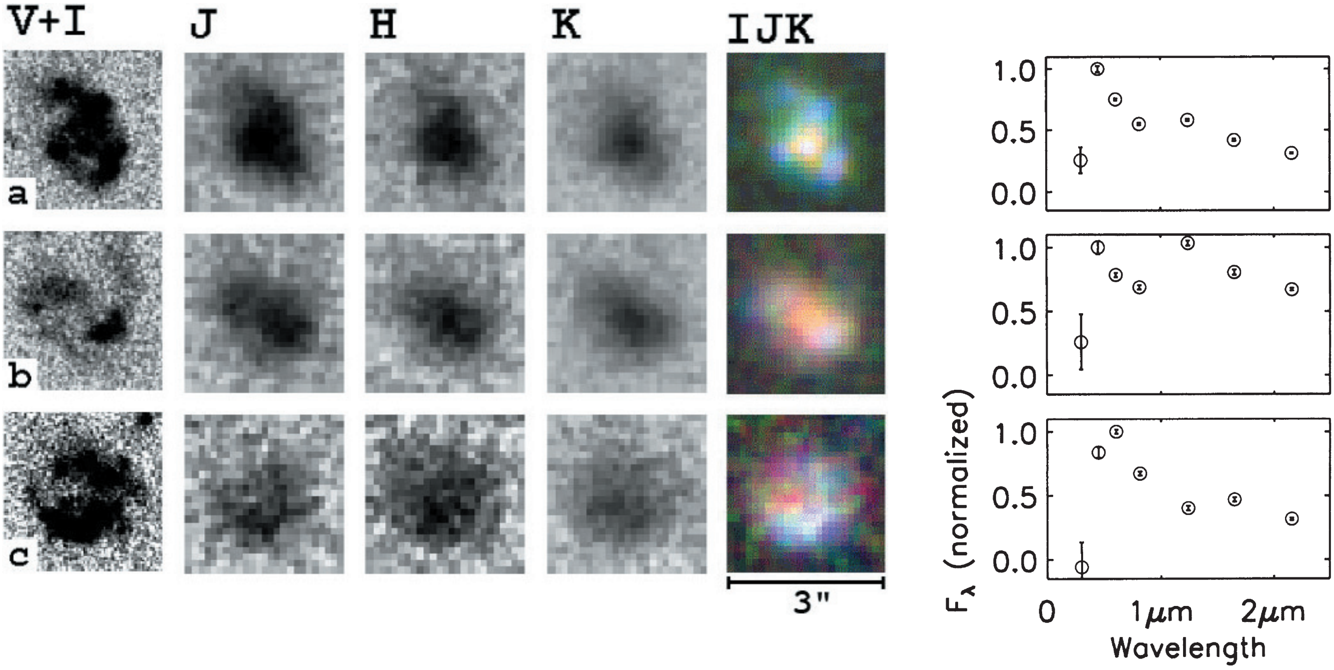

Figure 5: Same as Figure 3 for the three largest Lyman-break galaxies in the HDF-S. The K-band images (rest-frame optical) are more centrally concentrated than the WFPC2 images; this is a real change in light distribution and not caused by the decreased image quality in the NIR. The redshifts of galaxies (a) and (c) have been confirmed spectroscopically; they have z = 2.027 and z = 2.793 respectively, implying a scale length of $10h^{-1}$kpc for the latter.

Break galaxies over similar redshift ranges and with similar number densities. The overall properties of this red $J - K > 1.7$ strongly clustered population suggests that they are the progenitors of present-day massive ellipticals and extremely red objects (EROs) at $z \sim 1.5$.

5. Large Disk-Like Galaxies at High Redshift

The high-redshift galaxies in HDF-S show a large variation in both morphologies and spectral energy distributions. Spectacularly, we find some $z > 2$ galaxies that are very large in the rest-frame optical and show profound differences between the intrinsic ultraviolet and optical morphologies (Labbé et al. in preparation). Three of the galaxies, shown in Figure 5, are LBGs (selected by applying the U-dropout criteria of Madau et al. 1996), while one is the previously described red galaxy in Figure 3c. Their spectral energy distributions show a pronounced break in the rest-frame optical, identified as the age-sensitive Balmer/4000 Å break. They are amongst the brightest and reddest in the rest-frame optical and they are probably the most massive galaxies at $z \sim 2$–3.

The *I*-band morphologies (probing rest-frame 2000–2700 Å) are complex with a patchy distribution that is not concentrated towards the centre. Conversely, the NIR light is compact and peaks right in the centre of the *I*-band structure, surrounded by a diffuse and extended disk-like distribution. The most straightforward explanation is that these systems are very luminous giant spiral galaxies, with patchy star formation residing in a diffuse disk with a red bulge in the centre. It is well possible that we have discovered the predecessors of the large disk galaxies we see in the lower-redshift universe. Morphological studies in the rest-frame UV light of LBGs have always emphasized the compact and small sizes of the galaxies (Giavalisco et al. 1996, Lowenthal et al. 1997), as indeed is true for the bulk of our sample. However, galaxies that are large in the rest-frame optical with classical spiral morphologies have never been seen before, in particular not in the HDF-N (Dickinson et al. 2000) even though such structures would have been well recognizable in their deep WPFC2 and NICMOS imaging.

Follow-up VLT/FORS spectroscopy (Rudnick et al. 2002b in preparation) confirmed the redshift of the galaxy in Figure 5c, a disk-like U-dropout at $z_{spec} = 2.793 \pm 0.003$, implying a scale length of 10 h^{-1}kpc. Vanzella et al. (2002) found an identical redshift for this galaxy and for another, shown in Figure 5a, they found z_{spec} = 2.027. Theories of disk formation generally predict that large disk galaxies have been assembled recently ($z < 1$), and that high-redshift $z > 2$ disks are small and dense, with typical sizes of ~ few kpc. Producing large disk-like galaxies with reasonable likelihood may therefore pose a challenge to the current hierarchical models.

6. Summary

These first results on the HDF-S demonstrate the necessity of extending deep optical observations to near-IR wavelengths for a more complete census of galaxies in the early universe. In particular, the deepest-ever K_s-band data have proven to be invaluable, probing well into the rest-frame optical at $2 < z < 4$, where long-lived stars may dominate the light of galaxies.

Provided with a new window on the early universe we find previously undiscovered populations of galaxies, with possible far-reaching consequences for our understanding of galaxy formation. We find that the HDF-S has many more galaxies at $z \sim 3$ with very red $V_{606} - H$ colours than the HDF-N; these are candidates for relatively massive evolved systems. Closely connected, we find a substantial population of red $J_s - K_s > 2.3$ galaxies at $z > 2$, many of which are barely detectable even in the deepest optical images, and would be missed by optical colour selection techniques such as the U-dropout method. Yet, these galaxies probably contribute substantially to the total stellar mass present in the early universe at $z \sim 3$. We detect strong clustering ($r_0 = 8.3 \pm 1.2$ Mpc, comoving) of galaxies with $J_s - K_s > 1.7$ colours at $2 < z_{zphot} < 4$. The strong clustering and their red $J_s - K_s$ colours, suggest that there is a direct evolutionary link between these systems, EROs at $z \sim 1.5$, and massive elliptical galaxies in the local universe. We also find high-redshift systems that are very large in the rest-frame optical with morphologies similar to those of nearby giant spiral galaxies, containing a red bulge surrounded by a diffuse disk and with scattered patches of star-formation. While these are only a few examples, it is currently not clear whether galaxy formation models can produce objects of comparable colours and sizes in sufficient numbers to be consistent with our observations.

Lastly, the substantial differences between HDF-N and HDF-S demonstrate that results based on such small fields can be seriously affected by cosmic variance. The results of the second field in the FIRES survey, the much larger MS1054-03 field, should decide which one of the fields is atypical. We are pursuing extended follow-up programmes to obtain more spectroscopic confirmation of the above results, allowing us to fully investigate the nature of these galaxies and the clues they provide for models of galaxy formation. Updates on the FIRES programme and access to the reduced images and catalogues can be found at our website http://www.strw.leidenuniv.nl/~fires.

Acknowledgements

We wish to thank the ESO staff for operation of the VLT and ISAAC and their kind assistance. We are grateful for their enormous efforts in obtaining these data in service mode and making them available to us.

References

Moorwood, A.F.M., "ISAAC: a 1-5 μm imager/spectrometer for the VLT", in *Optical telescopes of today and tomorrow.* A.L. Ardeberg ed., *proc. SPIE* **2871**, pp. 1146–1151, 1997.

Steidel, C.C., Giavalisco, M., Dickinson, M., & Adelberger, K.L., *AJ* **112**, pp. 352-358, 1996.

Steidel, C.C., Giavalisco, M., Pettini, M., Dickinson, M., & Adelberger, K.L., *ApJ* **462**, L17, 1996.

Rudnick, G. et al., *AJ* **122**, pp. 2205–2221, 2001.

Labbé, I.F.L. et al., *AJ* accepted, 2002.

Förster Schreiber, N.M. et al., in preparation, 2002.

Oke, J.B. 1971, *ApJ*, **170**, 193.

Franx, M. et al., "FIRES at the VLT: the Faint InfraRed Extragalactic Survey", *The Messenger* **99**, pp. 20–22, 2000.

Casertano, S. et al., *AJ* **120**, pp. 2747–2824, 2000.

Papovich, C., Dickinson, M., & Ferguson, H.C., *ApJ* **559**, pp. 620–653, 2001.

Weinberg, D.H., Hernquist, L., & Katz, N., 2002, *ApJ*, **571**, 15.

Daddi, E. et al., *ApJ*, submitted, 2002.

Madau, P., Ferguson, H.C., Dickinson, M.E., Giavalisco, M., Steidel, C.C., & Fruchter, A., *MNRAS* **283**, pp. 1388–1404, 1996.

Giavalisco, M., Steidel, C. C., & Macchetto, F.D., *ApJ* **470**, 189, 1996.

Lowenthal, J.D. et al., *ApJ* **481**, pp. 673–688, 1997.

Rudnick, G. et al., in preparation, 2002a.

Rudnick, G. et al., in preparation, 2002b.

Dickinson, M., "The first galaxies: structure and stellar populations" *Philos. Trans. R. Soc. London* **A 358**, p. 2001, 2000.

Dickinson, M. et al., *ApJ* **531**, pp. 624–634, 2000.

Vanzella, E. et al., *A&A* accepted, 2002.

OTHER ASTRONOMICAL NEWS

Summary of the Workshop on

EXTRAGALACTIC GLOBULAR CLUSTER SYSTEMS

hosted by the European Southern Observatory in Garching on August 27–30, 2002

By M. KISSLER-PATIG

Extragalactic Globular Clusters, a Booming Field of Research

Globular cluster systems were established in the last decade as powerful tools for the study of galaxy formation and evolution. For this purpose they are used in nearby galaxies with as much success as the diffuse stellar populations and complement the latter studies by being superior in several practical aspects. For instance, globular clusters are better chronometers than the diffuse stellar population since each globular cluster can be identified as a single-age population. The age determination of the major globular cluster subpopulations allows one to precisely date the star formation events in the host galaxy.

Figure 1: NGC 6946 – a nearby spiral with a large number of very luminous young stellar clusters. Taken from Larsen's contribution. The observations were made with the ALFOSC instrument on the Nordic Optical Telescope on La Palma. ALFOSC is a twin instrument of DFOSC on the Danish 1.54-m and mounted on the NOT; it has a field size of about 6 × 6 arcmin. The colour image was generated from a mosaic of 3 pointings with red channel = V + I + Hα; green channel = V; blue channel = B.

Further, the study of globular cluster systems is the easiest way to detect multiple old or intermediate-age subpopulations within a galaxy. These in turn can trace multiple major star-formation episodes at early times, invisible in the studies of the diffuse galaxy light in which all populations are mixed.

Another advantage is that globular clusters can be traced far out in the halo, probing stellar populations and kinematics at several effective radii of the host galaxy – a range inaccessible to diffuse stellar light studies. The globular clusters can be used for dynamical studies at outer radii, shedding light on the assembly histories of the systems and the host galaxies.

Finally, globular clusters are very good calibrators at all wavelength for single stellar population models, an es-